



Article

Performance and Sensitivity Properties of Solid Heterogeneous Rocket Propellant Based on a Binary System of Oxidizers (PSAN and AP)

Katarzyna Gańczyk-Specjalska ^{1,*} , Paulina Paziewska ¹, Rafał Bogusz ¹, Rafał Lewczuk ¹, Katarzyna Cieślak ²  and Michał Uszyński ²

¹ Research Group of High Energetic Materials, Łukasiewicz Research Network–Institute of Industrial Organic Chemistry, Annopol 6, 03-236 Warsaw, Poland; paulina.magnuszewska@ipo.lukasiewicz.gov.pl (P.P.); rafal.bogusz@ipo.lukasiewicz.gov.pl (R.B.); rafal.lewczuk@ipo.lukasiewicz.gov.pl (R.L.)

² Division of High Energetic Materials, Warsaw University of Technology, Noakowskiego 3, 00-664 Warsaw, Poland; kcieslak@ch.pw.edu.pl (K.C.); mpj.uszynski@gmail.com (M.U.)

* Correspondence: katarzyna.ganczyk-specjalska@ipo.lukasiewicz.gov.pl

Abstract: Solid heterogeneous rocket propellants (SHRP) containing ammonium perchlorate (AP) emit a lot of hydrogen chloride (HCl) during combustion, which poses various environmental issues and makes the detection of the rockets easier. Part of the AP can be replaced by ammonium nitrate (V) (AN), which does not lead to the production of HCl. AN is a commonly used environmentally friendly oxidizer, but it is not usually applied in SHRP due to its disadvantages. One of these disadvantages is a phase transition near room temperature, which causes the density change of AN. Three types of phase stabilized ammonium nitrate (V) (PSAN) with inorganic potassium salts were obtained in order to shift this transition into higher temperatures (above the temperature range of the storage and the usage of SHRP). The SHRP with the PSAN were obtained, and the measurements of the heat of combustion, density, hardness, the sensitivity to mechanical stimuli and the thermomechanical properties were performed. The obtained propellants were characterized by similar operational parameters or were slightly lower than those without the PSAN. This means that AP can be partially replaced without significantly compromising the handling, safety or functionality of the propellants, while increasing the environmental performance of the solution.

Keywords: solid rocket propellant; phase stabilized ammonium nitrate (V); inorganic potassium salts; physical and thermomechanical properties of heterogeneous propellants



Citation: Gańczyk-Specjalska, K.; Paziewska, P.; Bogusz, R.; Lewczuk, R.; Cieślak, K.; Uszyński, M.

Performance and Sensitivity Properties of Solid Heterogeneous Rocket Propellant Based on a Binary System of Oxidizers (PSAN and AP). *Processes* **2021**, *9*, 2201. <https://doi.org/10.3390/pr9122201>

Academic Editor: Loïc Favregeon

Received: 8 November 2021

Accepted: 4 December 2021

Published: 7 December 2021

Publisher's Note: MDPI stays neutral with regard to jurisdictional claims in published maps and institutional affiliations.



Copyright: © 2021 by the authors. Licensee MDPI, Basel, Switzerland. This article is an open access article distributed under the terms and conditions of the Creative Commons Attribution (CC BY) license (<https://creativecommons.org/licenses/by/4.0/>).

1. Introduction

Ammonium nitrate (V) (AN) is widely used in both civil (e.g., mineral fertilizers) and military (e.g., solid rocket propellants) industries. The wide application of AN is due to its low price, high availability, safe usage, low sensitivity to mechanical stimuli or the absence of toxic combustion products. On the other hand, AN also has a number of disadvantages limiting its use, including its high hygroscopicity, low combustion velocity and the presence of a few phase transitions [1–5]. In order to limit the disadvantages (i.e., hygroscopicity, presence of phase transitions, low combustion velocity) of ammonium nitrate (V) in solid heterogeneous rocket propellants (SHRP), the following methods can be used [3–6]:

- The phase stabilization of ammonium nitrate (V);
- The modification of the AN surface to reduce the hygroscopicity;
- The addition of catalysts to increase the burning rate.

Ammonium nitrate has a minimum of five polymorphic transitions under atmospheric pressure below its melting temperature:

- Phase V, tetragonal, below $-16\text{ }^{\circ}\text{C}$;
- Phase IV, orthorhombic, $(-16)\text{--}32\text{ }^{\circ}\text{C}$;

- Phase III, orthorhombic, 32–84 °C;
- Phase II, tetragonal, 84–125 °C;
- Phase I, cubic, 125–170 °C [3,5].

Under microscopic observation, there are differences between the shapes of these phases: phase I—a shape “like plastic” without grain boundaries; phase II—large crystals; phase IV—highly heterogeneous with grain boundaries [7]. The most problematic phase transformation is the transition IV–III which occurs at 32 °C. The variation of ambient temperature and the repeated phase transitions causes the microcrystals separate to a fine powder. This transition is accompanied by a volume change of about 3.8%. The shift of volume and the structure of the crystals causes problems with the storage and the usage of AN-based materials. These changes lead to the deterioration of the mechanical properties and an increase of the porosity (surface). The structure of the solid rocket propellant based on AN is damaged when the material is subjected to temperature changes in the range of the phase transitions of AN between II and V [8]. Solid propellants containing such oxidants can crack during storage (due to the change in the AN volume caused by this transition), which may lead to a rough rocket motor operation, uncontrolled pressure build-up and even the explosion of the rocket combustion chamber [2,9]. There are various methods of AN phase stabilization that aim to extend the temperature range in which the transition from phase IV to III does not occur. Examples of the substances that cause the phase stabilization of AN are: inorganic and organic potassium salts [10,11], copper, zinc and nickel complexes [12,13], some organic compounds (e.g., melamine cyanurate, isatin, guanine) [14–16], etc. The phase stabilization of AN is carried out as a result of the co-crystallization of AN with an additive in an aqueous medium [12,17,18] or the addition of an additive in the melting process [8–11].

For example, the addition of manganese(IV) oxide, iron(III) oxide or their mixture to a propellant containing AN causes an increase in the burning rate up to 40% (at 7 MPa) in comparison to a propellant without these additives [6,17,19]. The introduction of metal nanoparticles increases the burning rate from 5% to 67% depending on the type of metal that is used [18]. With the appropriate modification of the composition of the solid heterogeneous rocket propellants, we have the ability to limit the unfavorable parameters and improve the ballistic properties.

Solid rocket propellants based on ammonium perchlorate are widely used. Such propellants emit significant amounts of hydrogen chloride during combustion. Hydrogen chloride has a negative impact on the environment, adversely affects the personnel operating the station and makes it easier to detect the rocket flight (a white smudge appears behind the nozzle). It is also worth noting that perchlorate ions are detected in soils and water [5] in various places around the world [5,20]. High concentrations of perchlorate ions negatively affect some body functions (e.g., the thyroid). Due to these negative effects, more work has been concerned with the possibility of replacing AP with other eco-friendly oxidants. AN seems to be a very good candidate due to its availability and the lack of negative environmental impacts.

The aim of this work was to obtain solid heterogeneous rocket propellants containing mixtures of oxidizers—ammonium perchlorate and phase stabilized ammonium nitrate (V) in order to reduce the amount of hydrogen chloride in the combustion products. The obtained samples were examined in terms of their sensitivity to mechanical stimuli, and their mechanical, physicochemical and thermal properties. The phase stabilization of the ammonium nitrate (V) was made before the formation of the propellants. Three potassium salts were used for this process: potassium nitrate (V) (PN), potassium carbonate (PC) and potassium perchlorate (PP). These salts were added in the amount of 5%. There are many studies concerning AN-based propellants, but there are few about AP-PSAN propellants. The novelty of this work is a result of the preparation of solid propellants containing: HTPB, AP-PSAN, Al and other additives for different AP/PSAN ratios than in the literature, as well as the characterization of the properties of these propellants in comparison to the AP-based propellant.

2. Materials and Methods

The following substances with a grade purity min. 95% were used to carry out the co-crystallization of the ammonium nitrate (V) with potassium salts: ammonium nitrate (V)—Chempur; potassium nitrate (V)—P.P.H. “Stanlab”; potassium carbonate—Chempur; potassium perchlorate—Chempur; ethyl acetate and distilled water.

The subsequent materials were used to obtain solid heterogenous rocket propellants: phase stabilized ammonium nitrate (V); hydroxyl-terminated polybutadiene (HTPB)—Island Pyrochemical Industries; dimeryl diisocyanate (DDI)—Island Pyrochemical Industries; dioctyl adipate (DOA)—Boryszew-Erg; lecithin (Lec)—Sigma-Aldrich; two fractions of ammonium perchlorate (AP): fine (AP_f , 80 μm) and coarse (AP_c , 250 and 400 μm)—Island Pyrochemical Industries; aluminum (Al, fraction of 32 μm)—Benda-Lutz. The size distribution of AP fine, AP coarse and Al is presented in Figure 1.

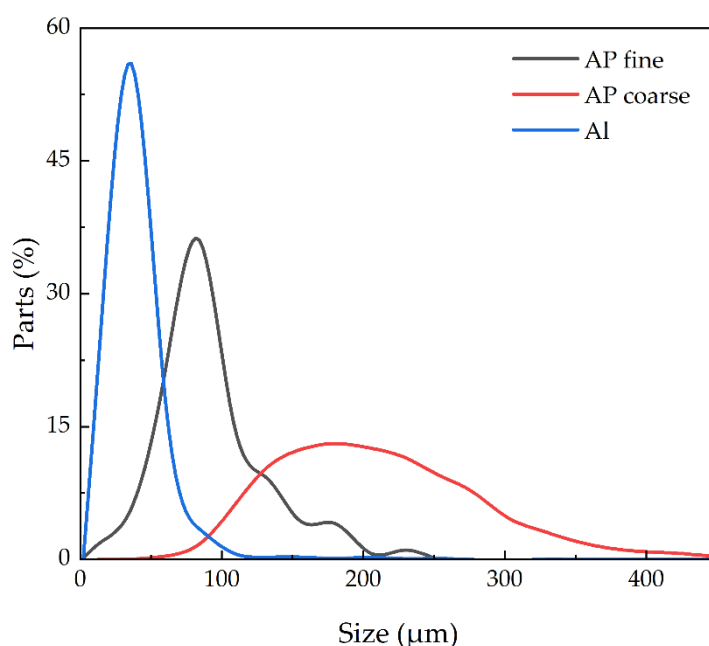


Figure 1. The size distribution of AP fine, AP coarse and Al.

There are many descriptions of AN phase stabilization methods in the literature [3,5,12,13,17,20]. The process of co-crystallization of ammonium nitrate (V) with salts and the optimal composition of the mixture of AN with potassium inorganic salt were based on the known examples [12,13,20].

In order to optimize the process, the following parameters were changed: the type of solvents (water, methanol, ethanol, acetone, ethyl acetate), the temperature, the dropping time and the speed of the agitator. The optimal conditions were selected after carrying out 15 processes. The description below complies with the optimal conditions of the co-crystallization process.

Ammonium nitrate (V) and selected potassium salt were placed in a three-necked flask (250 mL). Water (20 mL, ambient temperature) was added to 80 g of the binary mixture. The addition of water caused the mixture to partially dissolve, and then it was heated to 50–60 °C. The contents in the flask were mixed using a 4-blade stirrer. The speed of the agitator was gradually increased to 300 rpm and then held at this speed. It was mixed for an additional 10 min until the solids were completely dissolved. After this time, the temperature was slowly reduced to 10–15 °C. Simultaneously, ethyl acetate (40 mL) was added dropwise. The dropping time was 5–10 min. The precipitate was filtered under reduced pressure. Phase stabilized ammonium nitrate (V) (PSAN) was dried for 24 h at a

temperature of 70 °C. Three samples were obtained: AN + 5% potassium nitrate (V), AN + 5% potassium perchlorate and AN + 5% potassium carbonate. The process yield was min. 70%.

The process of formation of solid heterogenous rocket propellants was carried out in a laboratory planetary mixer NETZSCH PM with a capacity of 700 mL. The liquid components were added first: HTPB, DOA and lecithin. Next, aluminum powder and three fractions of oxidants (a fine fraction of AP, PSAN and a coarse fraction of AP) were added. Each oxidant was dried for at least 24 h in a dryer at 60 °C before the casting process to prevent the reaction of the curing agent with water. DDI (curing agent) was added at the end. Ingredients were mixed under atmospheric pressure and then under reduced pressure (10 mbar). The mixed propellant slurry was poured into a rectangular mold under reduced pressure. The composition of the reference propellant (SP0) was: 10.5% HTPB, 1.4% DOA, 0.1% Lec, 12.0% Al, 26.1% AP_f, 47.9% AP_c and 2.0% DDI. The composition of the propellants containing PSAN was: 10.5% HTPB, 1.4% DOA, 0.1% Lec, 12.0% Al, 10.0% AP_f, 42.9% AP_c, 21.1% PSAN and 2.0% DDI. Propellants with the PSAN addition were named as: SP-PN, SP-PP and SP-PC, which contained AN + 5%PN, AN + 5%PP and AN + 5%PC, respectively.

The particle size measurements of the phase stabilized ammonium nitrate (V) were performed using a Mastersizer 3000 from Malvern Instruments. The measurement was based on the laser diffraction method. The tests were carried out in chloroform with ultrasounds in order to break up any agglomerates. The samples were dried in an air-flow dryer at the temperature of 60 °C for minimum 2 h and then stored in a desiccator before the measurement.

The density of the samples was measured with an AccuPyc 1340 helium pycnometer at the temperature of 28 ± 1 °C.

Measurements of the heat of combustion were made with an IKA C2000 basic calorimeter. The mass of the propellant sample was 4.36 g and the mass of the standard propellant of the known combustion heat (4914 J/g) was 1.44 g. The pressure in the calorimetric vessel was reduced to 3–4 mbar. The standard propellant was used to ignite the propellant samples. Two measurements were performed for each sample and the average value was calculated.

The impact and friction sensitivity were determined with the BAM fall hammer and Peters apparatus, respectively. In both studies, sensitivity to an external stimulus is the lowest value of energy of impact or force of friction at which at least one positive result was obtained from six performed tests.

The hardness measurements were performed by a Shore durometer A-scale. Ten measurements were carried out for each sample. The average value for each propellant was calculated. Measurements were performed at the temperature of 25 ± 1 °C.

The study of thermochemical properties was performed by simultaneous differential thermal analysis and thermogravimetric analysis (DTA-TG) by the LabsysTM Evo (Setaram). The mass of the PSAN was 16 ± 1 mg and the mass of the propellants was 1.9 ± 0.2 mg. The samples were placed in open aluminum pans with a capacity of 30 µL. Measurements were made with a temperature increase rate of 5 °C/min in the temperature range from 30 to 500 °C in an argon flow. The measurements were performed at least three times for each sample. The following parameters were determined on the basis of the DTA-TG curves: onset temperature (T_{onset}), maximum temperature (T_{max}) and mass loss (Δm).

The analysis of the thermomechanical properties was carried out by dynamic mechanical analysis (DMA) by a DMA 242 Artemis apparatus (NETZSCH). A dual cantilever holder was used for the tests. The measurement was under nitrogen flow (50 mL/min) in the temperature range from -120 to 60 °C (the temperature increase rate was 2 °C/min). The rectangular propellant sample with the dimensions $50.0 \times 10.0 \times 2.0$ mm was subjected to vibrations with the frequencies of 0.5, 1.0, 2.0 and 5.0 Hz and a deformation amplitude of 20 µm during each measurement.

3. Results and Discussion

3.1. Influence of Potassium Salts on the Properties of Mixtures with Ammonium Nitrate (V)

Three processes of the phase stabilization of ammonium nitrate (V) with three different potassium salts were carried out. The obtained mixtures were tested with the DTA-TG analysis, density measurements and particle size measurements. Figure 2 shows the DTA-TG curves for pure ammonium nitrate (V). In the temperature range from 30 to 130 °C, endothermic transitions related to the change of the AN crystallographic form are observed. These are the phase transitions, respectively: IV(β) \rightarrow III(γ) with onset temperature $T_{onset} = 39.0$ °C and maximum temperature $T_{max} = 43.9$ °C; III(γ) \rightarrow II(δ) with $T_{onset} = 88.4$ °C and $T_{max} = 97.6$ °C; II(δ) \rightarrow I(ϵ) with $T_{onset} = 126.4$ °C and $T_{max} = 130.1$ °C. Next is the endothermic transition melting, which begins at $T_{onset} = 168.7$ °C ($T_{max} = 172.0$ °C). The complex endothermic transition that begins at the temperature above 200 °C with a mass loss associated with the decomposition of the AN. The total mass loss of the sample was $\Delta m = 88.2\%$.

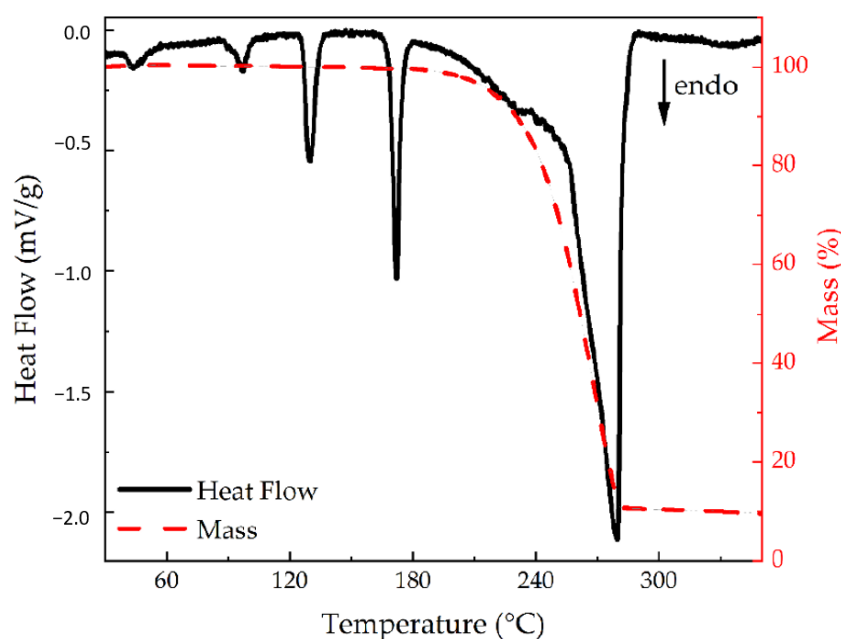


Figure 2. DTA-TG curves for ammonium nitrate (V).

Figure 3 presents the DTA curves of the pure AN and the AN modified with the potassium salts, while Table 1 summarizes the results of the DTA measurements. The applied potassium salts eliminated the IV \rightarrow III phase transition and did not affect the II \rightarrow I phase transition. Moreover, the potassium salts caused a shift of the III \rightarrow II phase transition towards higher temperatures. The melting process of all the PSAN mixtures shifted towards lower temperatures in comparison with the pure AN. Similar observations of the influence of the inorganic and the organic potassium salts on the phase transitions of AN can be found in the literature [5,11,21]. One of the reasons explaining the phase stabilization of AN at low temperatures is the partial replacement of ammonium cations with potassium cations as a result of the co-crystallization of AN with potassium salts.

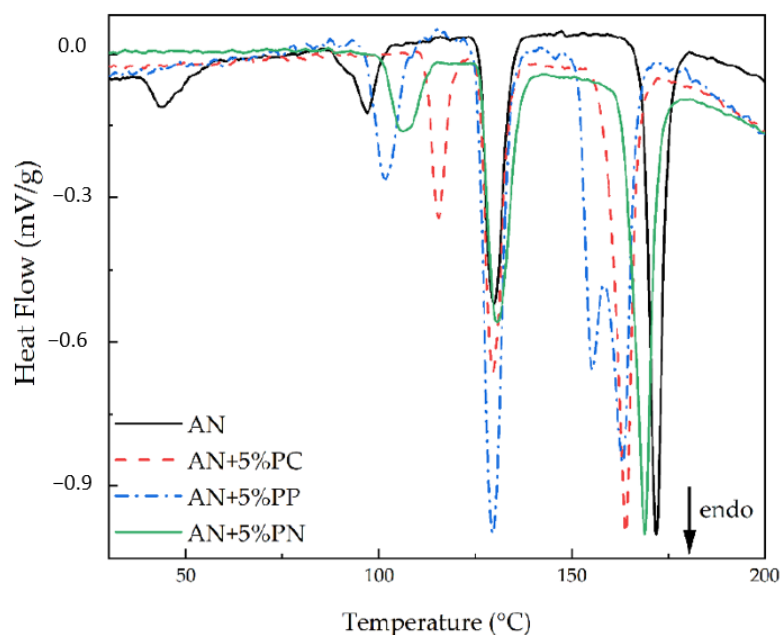


Figure 3. DTA-TG curves for AN and PSAN samples.

Table 1. Results from DTA-TG curves for AN and PSAN with various potassium salts.

Parameter		AN	AN + 5%PN	AN + 5%PP	AN + 5%PC
Δm^1 (%)		88.2	86.6	88.9	85.2
IV(β) \rightarrow III(γ)	T_{onset}^2 (°C)	39.0	-	-	-
	T_{max}^3 (°C)	43.9	-	-	-
III(γ) \rightarrow II(δ)	T_{onset} (°C)	88.4	101.0	95.6	112.4
	T_{max} (°C)	97.6	105.8	101.7	115.6
II(δ) \rightarrow I(ϵ)	T_{onset} (°C)	126.4	126.5	126.0	126.9
	T_{max} (°C)	130.1	131.1	130.1	130.4
Melting	T_{onset} (°C)	168.7	163.1	151.6	159.1
	T_{max} (°C)	172.0	169.1	163.2	164.4

¹ Mass loss; ² onset temperature; ³ maximum temperature.

The results of the density and particle size measurements of the PSAN with various potassium salts were gathered in Table 2. Mixtures of AN + 5%PP and AN + 5%PN are characterized by a similar density to pure AN (1.725 g/cm³ at 25 °C [5]). Only the AN + 5%PC mixture has a lower density. The modification of AN with potassium nitrate (V) resulted in particles with the smallest dimensions and the smallest deviation between the dimensions. The greatest difference between the dimensions was obtained for AN + 5%PP.

Table 2. Density and particle size of AN and PSAN with various potassium salts.

Parameter	AN + 5%PN	AN + 5%PP	AN + 5%PC
ρ^1 (g/cm ³)	1.714 \pm 0.001	1.710 \pm 0.005	1.677 \pm 0.002
$D_v(10)^2$ (μ m)	55 \pm 3	46 \pm 3	63 \pm 3
$D_v(50)^2$ (μ m)	132 \pm 5	155 \pm 3	152 \pm 4
$D_v(90)^2$ (μ m)	253 \pm 6	583 \pm 4	432 \pm 3

¹ Density; ² particle size for which x% of particles is below this value.

3.2. Properties of Solid Heterogeneous Rocket Propellants with Phase Stabilized Ammonium Nitrate (V)

The effect of the PSAN on the properties of the SHRP was determined with the ICT-Thermodynamic Code (version 1.00) program. The ICT-code uses mass action and mass balance expressions to calculate chemical equilibria. Thermodynamic equilibria can be estimated for constant pressure or volume conditions. The following settings were set: exclude gasses with mole numbers smaller than 10^{-5} ; start temperature for iterations—3000 K; step temperature iteration—20 K; freeze-out temperature—1500 K. The following parameters were compared: oxygen balance, density, heat of combustion, specific impulse and the mole fraction of hydrogen chloride (HCl) in gaseous products. Table 3 presents the obtained values. The heat of combustion was determined at a pressure of 0.1 MPa (the values include condensed water). The specific impulse and the composition of the combustion products were calculated for 7 MPa, and the expansion of the gaseous products for 0.1 MPa.

Table 3. Calculated parameters of SHRP with AP, AN and PSAN by ICT-code.

Parameter	SP0	SP0 + 20%AN	SP-PP	SP-PC	SP-PN
ρ^1 (g/cm ³)	1.728	1.689	1.692	1.692	1.690
OB ² (%)	−28.44	−31.25	−31.13	−31.61	−31.20
Q ³ (J/g)	6050	5675	5679	5609	5665
x_{HCl}^4 (%)	16.33	11.22	11.06	10.30	10.79
Isp ⁵ (s)	262.0	257.4	257.0	255.7	256.7

¹ Density; ² oxygen balance; ³ heat of combustion; ⁴ mole fraction of HCl; ⁵ specific impulse.

The addition of AN instead of AP to the propellants reduces all parameters, i.e., the density, the oxygen balance, the heat of combustion, the mole fraction of HCl and the specific impulse. The propellants with AN + 5%PP and AN + 5%PN have similar parameters. The addition of potassium carbonate causes a 37% reduction in the hydrogen chloride content in the combustion products in comparison with the SP0 composition. Simultaneously, it causes the greatest reduction in the combustion heat and specific impulse in the relation to the other propellants containing potassium salts.

The propellants were obtained by a casting method in keeping the same parameters of the technology process. The determined results of the properties are caused by the different properties of the samples, and not a different process of manufacturing. Table 4 presents the properties of the obtained propellants. All of the materials have a similar density, and their heat of combustion is lower than the parameter of the reference sample (SP0). There was no significant effect from the type of used potassium salt on the combustion heat, while the obtained experimental results were about 200 J/g higher than the calculated values (Table 3). The propellants with the PSAN have a similar sensitivity to the mechanical stimuli as to SP0. The highest hardness was obtained for SP-PP (47 °Sh), and the lowest for SP-PN (35 °Sh).

Table 4. Physicochemical properties and sensitivity to mechanical stimuli of obtained propellants.

Parameter	SP0	SP-PP	SP-PC	SP-PN
ρ^1 (g/cm ³)	1.708 ± 0.001	1.702 ± 0.002	1.699 ± 0.002	1.694 ± 0.001
Q ² (J/g)	6123 ± 40	5802 ± 29	5800 ± 34	5867 ± 42
IS ³ (J)	25	25	35	30
FS ⁴ (N)	120	160	120	120
H ⁵ (°Sh)	40 ± 2	47 ± 3	42 ± 5	35 ± 2

¹ Density; ² heat of combustion; ³ impact sensitivity; ⁴ friction sensitivity; ⁵ hardness Shore, scale A.

The thermal properties of the propellants were determined using the DTA-TG method. Figure 4 shows the curves for the SP-PN sample. The DTA curve shows a slight endothermic effect in the temperature range from 100 to 170 °C, which is related to the phase changes of the PSAN. There is no phase transition below 80 °C. A broad, complex exothermic transition begins above 200 °C with the mass loss of the sample. It is a complex decomposition process that consists of a series of overlapping endo- and exothermic processes. A clear endothermic peak at the temperature of 241 °C is associated with a change of the AP crystal form [22]. The mass loss can be divided into three stages: the first, above 135 °C, is related to the beginning of the propellant decomposition, and the second and third, in the range from 250 to 400 °C, are related to the further stages of the sample decomposition. Similar DTA-TG and TG-DTG curves were obtained for the other propellants. Table 5 presents the mass loss of the three stages and the onset and the maximum temperature of the decomposition peak. The presented values were averaged from the three comparable DTA-TG measurements.

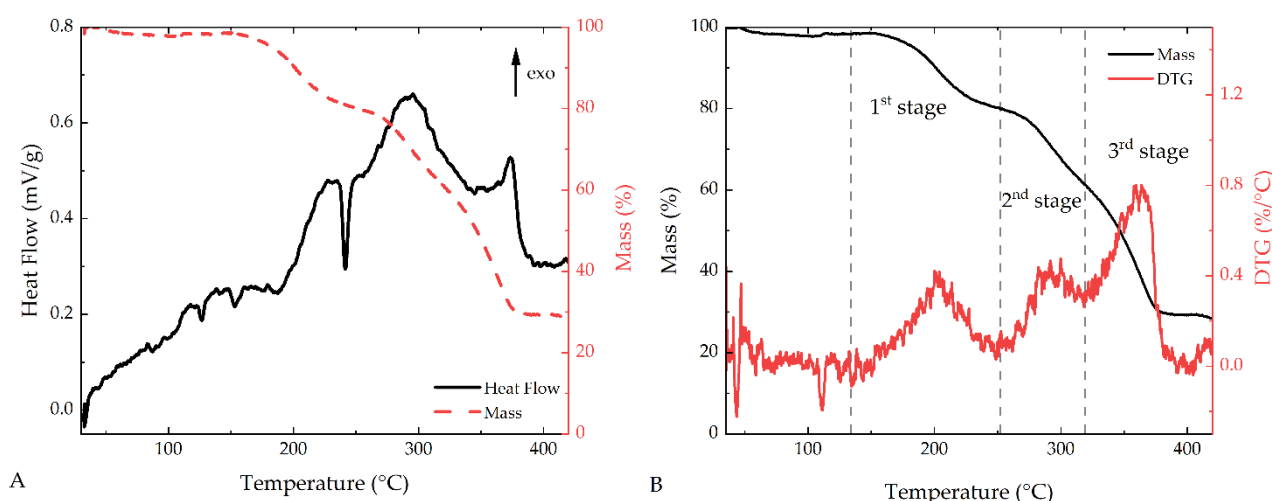


Figure 4. DTA-TG curve (A) and TG-DTG curve (B) for SP-PN propellant.

Table 5. Thermal properties of propellants.

Parameter	SP0	SP-PP	SP-PC	SP-PN
Δm_1^1 (%)	-	25 ± 2	23 ± 3	19 ± 2
Δm_2^2 (%)	-	16 ± 2	24 ± 4	19 ± 1
Δm_3^3 (%)	77 ± 6	32 ± 5	35 ± 3	32 ± 1
Δm^4 (%)	77 ± 6	73 ± 5	82 ± 4	70 ± 2
T_{onset}^5 (°C)	298 ± 3	191 ± 2	196 ± 2	197 ± 1
T_{max}^6 (°C)	320 ± 5	295 ± 1	295 ± 2	290 ± 3

¹ Mass loss of first stage; ² mass loss of second stage; ³ mass loss of third stage; ⁴ total mass loss; ⁵ onset temperature of main decomposition process; ⁶ maximum temperature of main decomposition process.

The total mass loss of the propellants SP-PP and SP-PN is slightly lower than the reference propellant SP0. The highest mass loss was determined for the propellant containing the PSAN modified by potassium carbonate. The maximum temperature of the decomposition process of the PSAN propellants is shifted towards the lower temperature by approx. 25 °C, and the onset temperature by approx. 100 °C in reference to the SP0 propellant. This means that the propellants containing two types of oxidants (AP and PSAN) are characterized by higher thermal sensitivity than the propellants containing only one oxidant—AP. The SP-PP, SP-PC and SP-PN propellants are characterized by similar parameters determined with the DTA-TG analysis. It can be concluded that the type of the

used potassium salts does not significantly affect the thermal properties of the decomposition process of the tested PSAN propellants. It should be noted that the beginning of the exothermic decomposition of all the PSAN-containing propellants begins at about 200 °C. These temperatures are above the temperatures used during the production process, which means that these propellants are safe for users. To assess the safety of the handling of these propellants, additional experiments should be performed in the future, such as the explosive response, the sensitivity to electrostatic discharge, artificial aging or compatibility.

The thermomechanical properties of the obtained propellants were characterized with the DMA method. The sample was placed in a dual cantilever holder and fixed at its ends, while the center part was moved. As a result of these vibrations, there are three areas of deformation in the sample: expansion, compression and shear. The obtained DMA curves consisted of three parameters: the storage modulus (E'), the loss modulus (E'') and the loss factor ($\tan\delta$). The DMA curves recorded for the SP-PP sample for the frequency of 1 Hz were presented in Figure 5. Similar DMA curves were obtained for the other propellants.

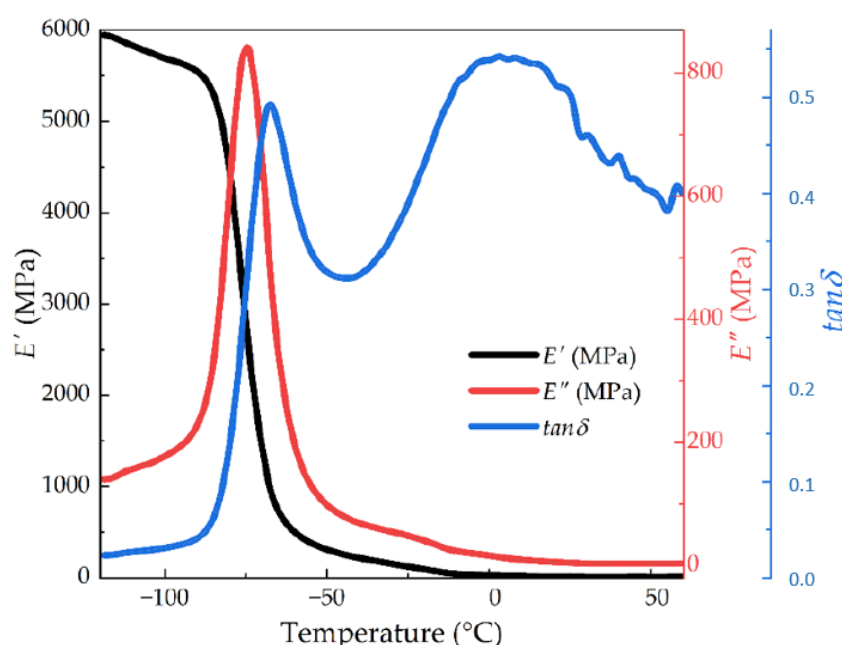


Figure 5. Storage modulus (E'), loss modulus (E'') and loss factor ($\tan\delta$) as a function of temperature for the SP-PP propellant ($f = 1$ Hz).

The obtained dependences of the E' , E'' and $\tan\delta$ parameters on the temperature are typical for SHRP containing polybutadiene [23–25]. The storage modulus decreases with an increasing temperature, from 5908 MPa (−115 °C) to 9 MPa (25 °C). From these curves, the glass transition temperature was determined as the onset point (−82.8 °C). The curve $E'' = f(T)$ shows a single peak at −74.6 °C ($E'' = 842$ MPa). Two peaks at −67.5 °C ($\tan\delta = 0.492$) and 3.1 °C ($\tan\delta = 0.543$) are observed on the loss factor curve. These two peaks are related to the presence of soft and hard segments in the polyurethane and the propellant. The movements of the HTPB polymer chain with unlimited mobility (first peak) are responsible for the soft segments. The urethane groups ($-N=C=O$) in the cross-linked HTPB are responsible for the hard segments. There are also soft segments with limited mobility due to the presence of solids and the interactions between the solids and the binder. Two effects overlap, and we observe them as the second peak [26–29]. Table 6 summarizes the glass transition temperatures of the obtained propellants, which were determined from the DMA curves.

Table 6. Glass transition temperatures of the propellants based on loss modulus and loss factor ($f = 1$ Hz).

Parameter	SP0	SP-PP	SP-PC	SP-PN
$T_g(E'')^1$ (°C)	−71.9	−74.6	−74.5	−77.0
$T_{g1}(\tan\delta)^2$ (°C)	−64.4	−67.5	−65.6	−67.5
$T_{g2}(\tan\delta)^3$ (°C)	−8.2	3.1	6.4	8.1

Glass transition temperature determined from: ¹ loss modulus curves; ² first peak of loss factor curves; ³ second peak of loss factor curves.

The glass temperature determined on the loss modulus and the loss factor curves are different—the temperature from the $E'' = f(T)$ curve is lower. The calculations based on $T_g(E'')$ are better because this temperature is connected with a loss of stiffness [30,31]. This approach is also recommended for solid rocket propellants in the STANAG 4540 standard [32]. The glass temperature of the propellants containing PSAN was lower by a minimum of 2.6 °C in regard to the SP0 propellant. The type of the used potassium salt in the PSAN did not significantly affect the glass temperature of the tested samples. The glass temperature of the hard segments for the PSAN propellants is higher by a minimum of 11 °C relative to the SP0 propellant. The type of the potassium salt influences the position of the second peak on the curve of the loss factor. The SP-PN sample was characterized by the highest glass temperature of the hard segments.

Figure 6 shows the dependencies of the particular DMA parameters for the different frequencies. All the curves shift towards higher temperatures with increasing frequency. The values of E' and $\tan\delta$ of the soft segments increase with the increase in the frequency, while the values of E'' and $\tan\delta$ of the hard segments decrease. The increasing frequency causes the polymer chains to have less time to adjust the mechanical energy as the sample temperature increases; therefore, the glass temperature shifts towards higher temperatures [33]. The determined values of the DMA parameters for the different frequencies are summarized in Supplementary Materials, Tables S1–S4.

The apparent activation energy was calculated based on the glass temperatures of the soft and hard segments from the $\tan\delta = f(T)$ curves according to the equation:

$$f = f_0 \cdot \exp\left(\frac{-E_a}{R \cdot T}\right) \quad (1)$$

where: f —frequency; f_0 —pre-exponential factor; E_a —apparent activation energy; R —general gas constant; T —temperature.

The apparent activation energy is connected with the energy of the intermolecular interactions during the phase transitions of the tested samples [33]. The calculated values of the apparent activation energies of the soft and hard segments are summarized in Table 7. The lowest values of E_a for the soft and hard segments were obtained for the SP-PC sample. The highest values of E_a for the soft segments were obtained for the SP-PP and SP-PN propellants. All of the calculated apparent activation energies of the hard segments obtained for the PSAN propellants differ from each other. This means that the PSAN changes the binder–solid phase interaction.

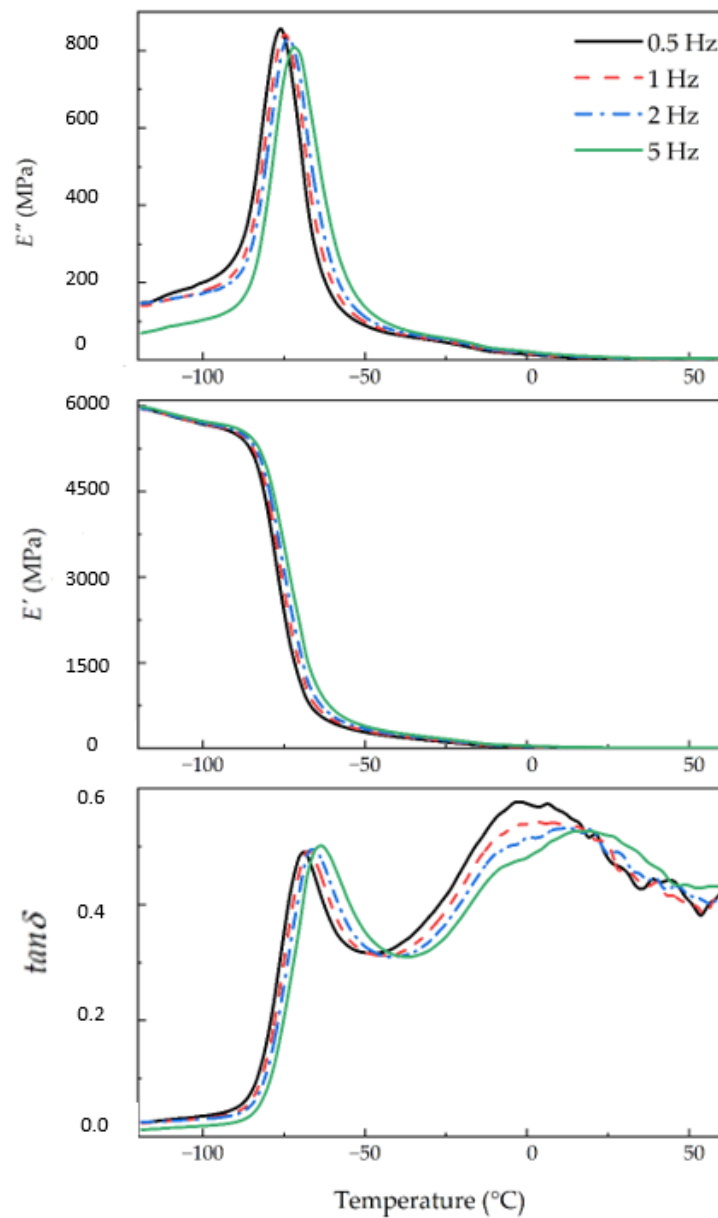


Figure 6. Dependences of storage modulus (E'), loss modulus (E'') and loss factor ($\tan\delta$) on the temperature for SP-PP propellant for different frequencies.

Table 7. Apparent activation energies and pre-exponential factors of soft and hard segments of obtained propellants.

Parameter	SP0	SP-PP	SP-PC	SP-PN
$aE_{a,soft}^1$ (kJ/mol)	149.6	156.9	144.4	157.5
$\ln f_{soft}^2$	86.1	91.7	83.7	92.2
$aE_{a,hard}^3$ (kJ/mol)	71.5	65.3	61.5	73.7
$\ln f_{hard}^4$	32.5	28.4	26.2	31.9

Apparent activation energy ¹ of soft and ³ hard segments. Natural logarithm of pre-exponential factor ² of soft and ⁴ hard segments.

4. Conclusions

In this work, the experimental and calculated performance of solid heterogeneous propellants containing a binary system of oxidizers (AP and PSAN) was presented. Phase stabilized ammonium nitrate (V) was obtained as a result of the co-crystallization with inorganic potassium salts: nitrate (V), carbonate and perchlorate, and the obtained PSAN had no phase transitions in the temperature range from 30 to 85 °C. The reduction in the volume of hydrogen chloride in the combustion products by 32–37% was observed in the obtained propellants. Some of the parameters of these materials are similar to the AP-based propellants. Other parameters, like the heat of combustion or the specific impulse, are lower in comparison to the reference propellant. For this reason, the new compositions can be used for, e.g., gas generators or training loads. The obtained propellants can be also modified by additional components in order to improve the selected parameters and to extend their possible applications.

Supplementary Materials: The following are available online at <https://www.mdpi.com/article/10.3390/pr9122201/s1>, Table S1: Results from DMA curves for SP0 propellant; Table S2: Results from DMA curves for SP-PN propellant; Table S3: Results from DMA curves for SP-PP propellant; Table S4: Results from DMA curves for SP-PC propellant.

Author Contributions: Conceptualization, K.G.-S., P.P. and R.B.; methodology, K.G.-S. and R.B.; validation, R.L. and K.C.; formal analysis, R.L.; investigation, M.U., P.P. and K.G.-S.; resources, P.P.; data curation, R.B.; writing—original draft preparation, K.G.-S., R.B. and R.L.; writing—review and editing, K.G.-S.; visualization, K.C.; funding acquisition, K.G.-S. All authors have read and agreed to the published version of the manuscript.

Funding: This research was funded by The National Centre for Research and Development under the scientific research program for national defense and security, “Future technologies for defence—Young Scientists Competition”, grant number DOB-2P/03/01/2018.

Institutional Review Board Statement: Not applicable.

Informed Consent Statement: Not applicable.

Data Availability Statement: The data is contained within this article.

Conflicts of Interest: The authors declare no conflict of interest.

References

1. Trache, D.; Klapötke, T.M.; Maiz, L.; Abd-Elghany, M.; DeLuca, L.T. Recent Advances in New Oxidizers for Solid Rocket Propulsion. *Green Chem.* **2017**, *19*, 4711–4736. [\[CrossRef\]](#)
2. Oommen, C.; Jain, S.R. Ammonium Nitrate: A Promising Rocket Propellant Oxidizer. *J. Hazard. Mater.* **1999**, *67*, 253–281. [\[CrossRef\]](#)
3. Chaturvedi, S.; Dave, P.N. Review on Thermal Decomposition of Ammonium Nitrate. *J. Energetic Mater.* **2013**, *31*, 1–26. [\[CrossRef\]](#)
4. Sinditskii, V.P.; Egorchev, V.Y.; Tomasi, D.; Deluca, L.T. Combustion Mechanism of Ammonium-Nitrate-Based Propellants. *J. Propuls. Power* **2008**, *24*, 1068–1078. [\[CrossRef\]](#)
5. Jos, J.; Mathew, S. Ammonium Nitrate as an Eco-Friendly Oxidizer for Composite Solid Propellants: Promises and Challenges. *Crit. Rev. Solid State Mater. Sci.* **2017**, *42*, 470–498. [\[CrossRef\]](#)
6. Naya, T.; Kohga, M. Burning Characteristics of Ammonium Nitrate-Based Composite Propellants Supplemented with MnO₂. *Propellants Explos. Pyrotech.* **2013**, *38*, 87–94. [\[CrossRef\]](#)
7. Dunuwille, M.; Yoo, C.S. Phase Diagram of Ammonium Nitrate. *J. Chem. Phys.* **2013**, *139*, 214503.1–214503.11. [\[CrossRef\]](#)
8. Maggi, F.; Garg, P. Fragmentation of Ammonium Nitrate Particles under Thermal Cycling. *Propellants Explos. Pyrotech.* **2018**, *43*, 315–319. [\[CrossRef\]](#)
9. Babrauskas, V.; Leggett, D. Thermal Decomposition of Ammonium Nitrate. *Fire Mater.* **2020**, *44*, 250–268. [\[CrossRef\]](#)
10. Oommen, C.; Jain, S.R. Phase Modification of Ammonium Nitrate by Potassium Salts. *J. Therm. Anal. Calorim.* **1999**, *55*, 903–918. [\[CrossRef\]](#)
11. Xu, Z.-X.; Fu, X.-Q.; Wang, Q. Phase Stability of Ammonium Nitrate with Organic Potassium Salts. *Cent. Eur. J. Energetic Mater.* **2016**, *13*, 736–754. [\[CrossRef\]](#)
12. Sudhakar, A.O.R.; Mathew, S. Thermal Behaviour of CuO Doped Phase-Stabilised Ammonium Nitrate. *Thermochim. Acta* **2006**, *451*, 5–9. [\[CrossRef\]](#)

13. Mathew, S.; Krishnan, K.; Ninan, K.N. A DSC Study on the Effect of RDX and HMX on the Thermal Decomposition of Phase Stabilized Ammonium Nitrate. *Propellants Explos. Pyrotech.* **1998**, *23*, 150–154. [[CrossRef](#)]
14. Golovina, N.I.; Nechiporenko, G.N.; Nemtsev, G.G.; Dolganova, G.P.; Roshchupkin, V.P.; Lempert, D.B.; Manelis, G.B. Phase State Stabilization of Ammonium Nitrate for Creating an Oxidizing Agent for Smokeless Gas-Generating Formulations Yielding No Toxic Combustion Products. *Russ. J. Appl. Chem.* **2007**, *80*, 24–30. [[CrossRef](#)]
15. Golovina, N.; Nechiporenko, G.; Nemtsev, G.; Zyuzin, I.; Manelis, G.B.; Lempert, D. Ammonium Nitrate Phase State Stabilization with Small Amounts of Some Organic Compounds. *Cent. Eur. J. Energetic Mater.* **2009**, *6*, 45–56.
16. Lee, T.; Chen, J.W.; Lee, H.L.; Lin, T.Y.; Tsai, Y.C.; Cheng, S.L.; Lee, S.W.; Hu, J.C.; Chen, L.T. Stabilization and Spheroidization of Ammonium Nitrate: Co-Crystallization with Crown Ethers and Spherical Crystallization by Solvent Screening. *Chem. Eng. J.* **2013**, *225*, 809–817. [[CrossRef](#)]
17. Kohga, M. Thermal Decomposition Behaviors and Burning Characteristics of Ammonium Nitrate/Polytetrahydrofuran/Glycerin-Based Composite Propellants Supplemented with MnO₂ and Fe₂O₃. *Propellants Explos. Pyrotech.* **2017**, *42*, 665–670. [[CrossRef](#)]
18. Gromov, A.A.; Popenko, E.M.; Sergienko, A.V.; Slyusarsky, K.V.; Nalivaiko, A.Y.; Ozherelkov, D.Y.; Larionov, K.B.; Dzidziguri, E.L. Characterization of Aluminum Powders: IV. Effect of Nanometals on the Combustion of Aluminized Ammonium Nitrate-Based Solid Propellants. *Propellants Explos. Pyrotech.* **2021**, *46*, 450–459. [[CrossRef](#)]
19. Naya, T.; Kohga, M. Burning Characteristics of Ammonium Nitrate-Based Composite Propellants Supplemented with Fe₂O₃. *Propellants Explos. Pyrotech.* **2013**, *38*, 547–554. [[CrossRef](#)]
20. Nadaraja, A.V.; Puthiyaveetil, P.G.; Bhaskaran, K. Surveillance of Perchlorate in Ground Water, Surface Water and Bottled Water in Kerala, India. *J. Environ. Health Sci. Eng.* **2015**, *13*, 1–6. [[CrossRef](#)]
21. Kaniewski, M.; Hoffmann, K.; Hoffmann, J. Influence of Selected Potassium Salts on Thermal Stability of Ammonium Nitrate. *Thermochim. Acta* **2019**, *678*, 178313. [[CrossRef](#)]
22. Boldyrev, V.V. Thermal Decomposition of Ammonium Perchlorate. *Thermochim. Acta* **2006**, *443*, 1–36. [[CrossRef](#)]
23. Seyidoglu, T.; Bohn, M.A. Characterization of Aging Behavior of Butacene[®] Based Composite Propellants by Loss Factor Curves. *Propellants Explos. Pyrotech.* **2017**, *42*, 712–723. [[CrossRef](#)]
24. Gao, W.; He, J.; Xiao, F.; Yang, R. Synthesis of Propargyl-Terminated Polybutadiene and Properties of Polytriazole Elastomers. *Propellants Explos. Pyrotech.* **2019**, *44*, 1183–1192. [[CrossRef](#)]
25. Bihari, B.K.; Wani, V.S.; Rao, N.P.N.; Singh, P.P.; Bhattacharya, B. Determination of Activation Energy of Relaxation Events in Composite Solid Propellants by Dynamic Mechanical Analysis. *Def. Sci. J.* **2014**, *64*, 173–178. [[CrossRef](#)]
26. Cerri, S.; Bohn, M.A.; Menke, K.; Galfetti, L. Aging of HTPB/Al/AP Rocket Propellant Formulations Investigated by DMA Measurements. *Propellants Explos. Pyrotech.* **2013**, *38*, 190–198. [[CrossRef](#)]
27. Cerri, S.; Bohn, M.A.; Menke, K.; Galfetti, L. Ageing Behaviour of HTPB Based Rocket Propellant Formulations. *Cent. Eur. J. Energetic Mater.* **2009**, *6*, 149–165.
28. de la Fuente, J.L.; Rodríguez, O. Dynamic Mechanical Study on the Thermal Aging of a Hydroxyl-Terminated Polybutadiene-Based Energetic Composite. *J. Appl. Polym. Sci.* **2003**, *87*, 2397–2405. [[CrossRef](#)]
29. Young, R.J.; Lovell, P.A. Elastomers. In *Introduction to Polymers*, 2nd ed.; Springer Science+Business Media: Hong Kong, China, 1991; pp. 300–306.
30. Akay, M. Aspects of Dynamic Mechanical Analysis in Polymeric Composites. *Compos. Sci. Technol.* **1993**, *47*, 419–423. [[CrossRef](#)]
31. Li, G.; Lee-Sullivan, P.; Thring, R.W. Determination of Activation Energy for Glass Transition of an Epoxy Adhesive Using Dynamic Mechanical Analysis. *J. Therm. Anal. Calorim.* **2000**, *60*, 377–390. [[CrossRef](#)]
32. Eriksen, J.H. *Explosives, Procedures for Dynamic Mechanical Analysis (DMA) and Determination of Glass Transition Temperature*; STANAG 4540 Ed. 1; North Atlantic Treaty Organization: Brussels, Belgium, 2002.
33. Lemos, M.F.; Bohn, M.A. DMA of Polyester-Based Polyurethane Elastomers for Composite Rocket Propellants Containing Different Energetic Plasticizers. *J. Therm. Anal. Calorim.* **2018**, *131*, 595–600. [[CrossRef](#)]